INDIAN JOURNAL OF SCIENCE AND TECHNOLOGY

RESEARCH ARTICLE

Electrical and Raman Spectroscopic Studies on Gd-Modified Strontium Bismuth Titanium Zirconium Oxide

C Jyothirmai[1], N V Prasad[2]*

1 Research Scholar, Material Research Laboratory, Department of physics, Osmania University, Hyderabad, Telangana, India
2 Associate Professor, Material Research Laboratory, Department of Physics, Osmania University, Hyderabad, Telangana, India

OPEN ACCESS

Received: 08-03-2024

Accepted: 08-07-2024

Published: 12-08-2024

Citation: Jyothirmai C, Prasad NV (2024) Electrical and Raman Spectroscopic Studies on Gd-Modified Strontium Bismuth Titanium Zirconium Oxide. Indian Journal of Science and Technology 17(32): 3296-3304. https://doi.org/10.17485/IJST/v17i32.675

* **Corresponding author**.

nvp1969@rediffmail.com

Funding: None

Competing Interests: None

Published By Indian Society for Education and Environment (iSee)

ISSN
Print: 0974-6846
Electronic: 0974-5645

Abstract

Objectives: The work is focused on the electrical properties of rare earth (Gd^{3+}) modified strontium titanate ($Gd_xSrBi_{4-x}Ti_{3.85}Zr_{0.15}O_{15}$; x=0.15, 0.25, and 0.50) novel ceramics to understand the plausible reason for dielectric relaxations in IR region. **Methods:** The above compounds were prepared by conventional solid-state route. Crystalline information was obtained by X-ray diffraction patterns. The distribution of Gd ion into the $(Bi_2O_2)^{2+}$ bismuth oxide layer was studied by Raman spectroscopic analysis. Impedance and dielectric measurements were performed, using an impedance analyzer, model Auto-Lab PGSTAT30 and NOVA11.1. A detailed electrical analysis was adopted to understand the inherited electrical properties of the materials. **Findings:** The surface morphology was found to be a plate-like structure. The grain size was found to decrease with increasing the Gd^{+3} content in the lattice. The SGBT-0.50 sample has shown a transition temperature of around 500°C. Temperature impedance spectroscopic plots have shown dielectric relaxations. The spectroscopic peak maximum is found to shift towards the higher frequency side with increasing temperature. The spectroscopic data is compared to the dielectric and Raman modes. Based on the high conductivity at higher temperatures, it clearly indicates that these ceramics can be useful dielectrics for high-temperature applications. **Novelty:** The activation energy, calculated from the electrical studies, and the high gran resistance suggests the involvement of ionization of oxygen vacancies in the conduction process. A detailed conductivity analysis using Jonscher's Universal law confirms the same. We have come across a few reports on magnetic ions namely Gd in bismuth-layered structure ferroelectric (BLSF) ceramics. In this paper, we have discussed the fabrication of compounds, structural information, dielectric, impedance and AC-conductivity properties.

Keywords: Solid - state reaction method; XRD; Raman; Impedance; Dielectric constant

1 Introduction

Ferroelectric materials have been attracted owing to the fact of its hysteresis behavior. They provide new freedom for the design of FRAM devices for speed reading and writing [1]. It is a known fact that ferroelectricity arises due to the space inversion of symmetry breaking. Recent reports on magnetic and electric ordering enable in perovskites made a new hallmark, especially in Aurivillius multiferroic materials [2]. Rare earth materials like La^{3+}, Sm^{3+}, Dy^{3+} and Y^{3+} doped $BaTiO_3$ have shown improved ferroelectric properties. However, high concentration RE-doped $BaTiO_3$ materials have shown high conductivity and inhibit the grain growth mechanism. Therefore, low concentration of rare earth modified bismuth ferrite (RE-$BiFeO_3$) samples are being prepared for tunable electrical properties [2]. Aurivillius phase layered-perovskite materials, known as bismuth layered structure ferroelectric (BLSF) are considered to be alternatives to $BaTiO_3$, lead-free and single phase promising ferroic materials [2,3]. Strontium bismuth titanate (SBT), is the most adaptable member of the layered perovskite family and has several special qualities, like high temperature piezoelectric materials and memory-storage devices, high curie temperature, a high dielectric constant, and low dielectric loss [3–5]. The chemical formula for the present layered-perovskite of the Aurivillius family is $(A_{m-1}B_mO_{3m+1})^{2-}$. The perovskite blocks shown in the bracket term are inter-leaved with $(Bi_2O_2)^{2+}$ layers. Here A-is RE/Bi with 12-coordination site and B is Ti/Zr with 6-coordination site. The term n indicates the number of layers or perovskite units. SBT ceramic has a high curie temperature (540°C), with orthorhombic group $A2_iam$. Above the transition temperature, the compound terns into tetragonal space group 14/mm [5,6]. The major drawback of SBT is its bismuth volatization during the solid-state sintering process. The bismuth volatization creates oxygen vacancies and these vacancies play a role in maintaining charge neutrality conditions. Moreover, the oxygen vacancies play an important role in electric properties. It is reported that the diffusion of oxygen vacancies pin the domain wall and subsequently enhances the leakage currents. In order to decrease the leakage currents, many researchers have reported SBT with different ion modifications in A-and B-sites. It is a known fact that Zr- modification in place of Ti for B-site enhances the ferroelectric properties. A-site, B-site, and both A- and B-site SBT reports are widely accessible and have garnered significant attention due to their improved electrical properties. Nayak et al. revealed the properties of Zr-modified SBT ceramics, which result in structural distortion and significantly change electrical properties [7–9].

Based on our recent reports and in the literature, Sr $Bi_4Ti_{3.85}Zr_{0.15}O_{15}$ is shown to be a more promising layer-perovskite [6–8]. However, rare earth, such as La/Sm, modified SBT has shown good ferroelectric properties. Many researchers have reported that the magnetic ions such as Fe/Co modified Ti (B-site) and rare earth (La, Sm) modified for Bi-(A-site) have shown lower conductivity and governed the electrical properties. Keeping this in view, the high magnetic moment rare earth (Gd^{+3}) modified SBTZ is prepared in the present investigation with a different Gd^{+3}composition. In this work, the detailed impedance and conductivity properties of SBTZ was studied. To the best of our knowledge, Gd modified SBTZ is not reported so far.

2 Methodology

2.1. Sample preparation and characterization

The traditional solid-state reaction approach was used to create the Gd (rare earth) modified composition $SrR_xBi_{4-x}Ti_{3.85}Zr_{0.15}O_{15}$ of (x=0.15, 0.25, 0.50) ceramics. The nomenclature of the composition is SGBTZ-0.15, SGBTZ-0.25, SBTZ-0.50. High-purity oxides of $SrCO_3$, Bi_2O_3, TiO_2, Gd_2O_3, and ZrO_2 were employed as the starting materials in this procedure. A ball mill was used to ground the oxide reactant mixture.

These oxides were extensively ground in a planetary ball mill with ethanol medium for duration of 12 hours. Furthermore, a 2% surplus Bi_2O_3 was included into the mixture to compensate for the bismuth loss during the sintering procedure.

The mixture was calcined for a duration of four hours at 850°C. After the ball milled, the calcined powder was combined with a binder (3% PVA). For the production of pellets, the powder was compressed using hydraulic pressure into circular discs with a 10 mm diameter and 1 mm thickness. The pellets were pre-sintered in a conventional furnace for four hours at 900°C.

Using an analytical X-ray diffractometer, phase analysis was performed on all samples and the results were compared to those of the standard compound SBTZ, ICSD #51863. Using Powd software, compounds lattice properties were calculated. Using a scanning electron microscope (SEM) model CARLZEISS-EVO18SEM, surface morphology was examined. Auto-Lab PGSTAT30 and NOVA11.1 were utilized to measure impedance data of all samples. Impedance results were corroborated by the Raman data.

3 Results and Discussions

All samples exhibited an XRD pattern with no extra peaks, indicating the lack of an impurity phase for the produced materials. The highest intensity peak measured at plain index and 30° range is (119). All samples of SGBTZO exhibit a modest shift with respect to the maximum peak towards the high range with an increase in doping material concentration. The calculated lattice parameters, Orthorhombic distortion and volume of all samples were listed in Table 1. The presence of (0 0 l) plane clearly indicates the preferential growth along C-axis. The lattice parameters were calculated through powd software, considering $A2_i$ am orthorhombic space group of parent compound (SBT), A decease of lattice parameters, compared to parent compound SBTZ clearly indicates that Gd readily occupies the bismuth oxide layer and brings charges in TiO_6 octahedra tilt [8–10].

The degree of a-axis orientation ($\propto$) can be measured with the help of following equation:

$$\propto = \frac{I(00l)}{I(119) + I(hkl)}$$

I (00*l*), I (119) and I (hkl) represent the XRD intensities observed at those particular reflections. From this it is evident that the crystal structure tunes from orthorhombic to tetragonal or pseudo- orthorhombic.

Scanning electron microscope (SEM) pictures give information about the material's microstructure and surface shape. SEM pictures consist of more or less plate-like structures and the grain size decreases with increasing the Gd concentration. Since (0 0 l) planes possess lower surface energy, crystal growth occurs along ab-direction during sintering, grain morphology attains plate-like morphology with increasing Gd concentration. The plate-like morphology transforms into circular shaped grains with rounded edges and therefore the grain size decreases (see Table 1). The histogram representation of grains found in different regions is plotted with the help of image J software as shown as inset Figure 2. From this it is evident that Gd^{3+} ion acts as a grain growth inhibitor. More aspect of this could be discussed later.

Table 1. The lattice parameter, orthorhombic distortion, volume values of SGBTZO-x (where x=0.15, 0.25, 0.50)

Composition	Lattice parameters			Orthorhombic distortion	Grain size
	a(Å)	b(Å)	c(Å)	b/a	μm
SGBTZO-0.15	5.450	5.428	40.984	0.995	0.37
SGBTZO-0.25	5.454	5.426	40.984	0.994	0.433
SGBTZO-0.50	5.454	5.425	41.945	0.994	0.33

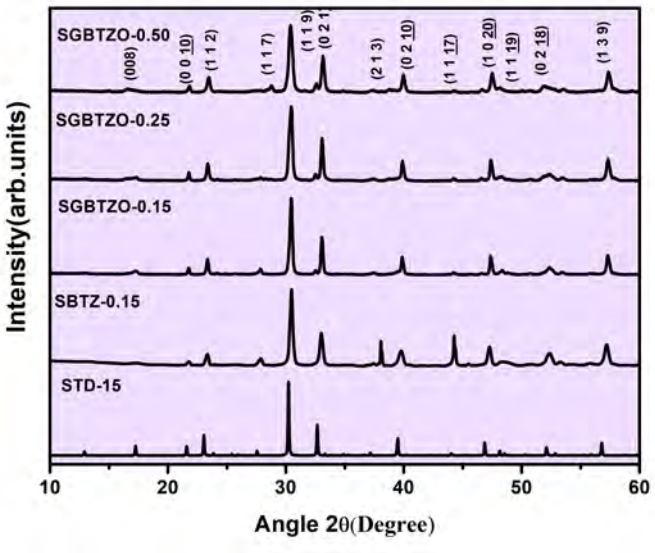

Fig 1. XRD pattern of SGBTZO-x (x=0.15, 0.25, 0.50)

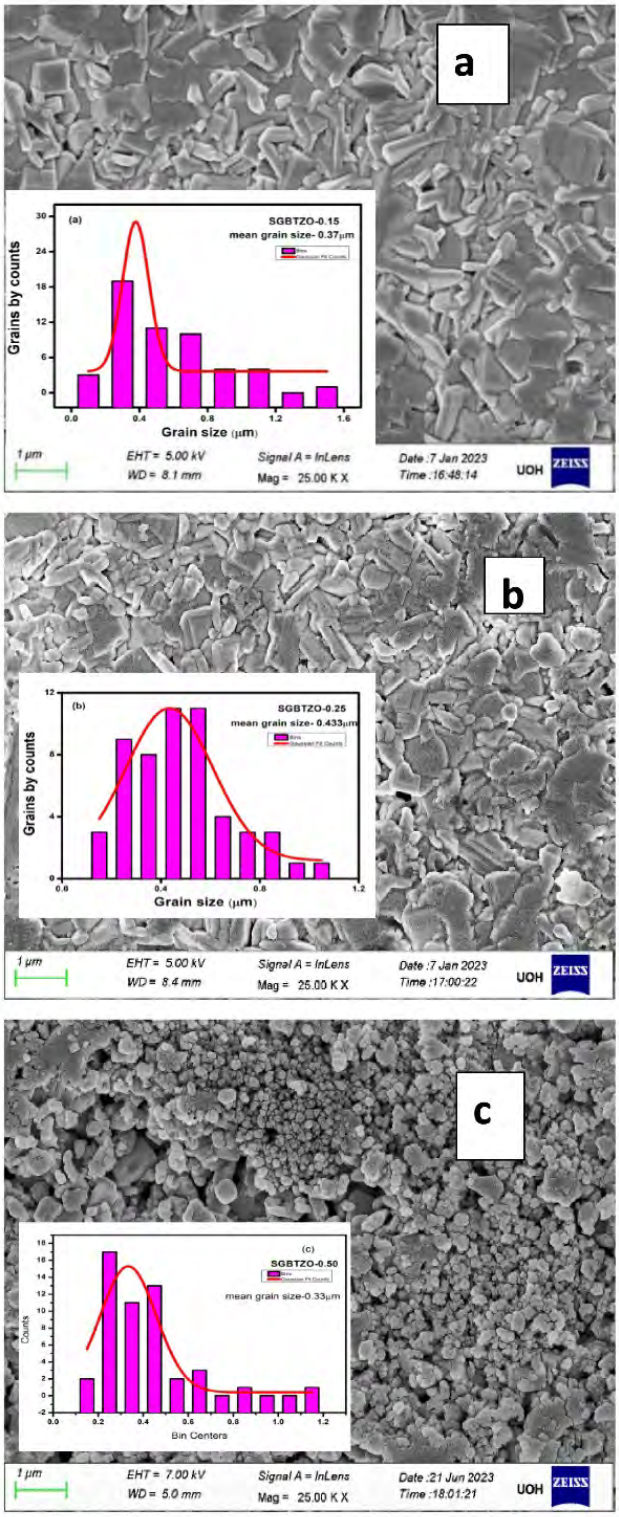

Fig 2. (a-c) SEM images of SGBTZO-x (x=0.15, 0.25, 0.50)

The Raman spectrum of Gd-modified SBTZO is shown in Figure 3**(a-c).** Based on the structural chemistry point of view, the orthorhombic structure of the present set of compounds has the following two types of vibrational modes viz.(i) internal mode of TiO_6 octahedral (ii) lattice cation translation modes of perovskite and bismuth oxide layers. The sharp phonon modes at ~ 100,265,550,860cm^{-1} and few weak modes near 100,320,470 cm^{-1} were observed. All the characteristic modes of SBT already have been reported by several researchers [9–11]. Low frequency modes of SBT were found at 155 cm^{-1}. However, in the present investigation mode observed near 100 cm^{-1} clearly indicates that Gd^{+3} ion readily substitutes Bi^{+3}ion. Low frequency modes are generally considered the heavier ion Bi^{+3}/Gd^{+3} vibrational mode or also called rigid-layer mode. The hump-mode observed near 150cm^{-1}corresponds to A-site ion namely Bi^{+3} and Gd^{+3}. The Raman modes observed above 260cm^{-1} correspond to TiO_6 octahedral and such intense strong mode corresponds rocking mode. This mode is observed due to the torsional bending of TiO_6 octahedral. The mode observed near 860 cm^{-1} is called stretching mode of TiO_6 octahedral [10]. A slight deviation is observed in all the modes. Mode frequency is found to increase with increasing the Gd concentration. This observation is consistent to the mass ratio of Bi/Gd. As the mass of Gd increases, then the mode frequency is found to shift towards lower frequency sides. Similar results were reported by Nayak et al. [5].

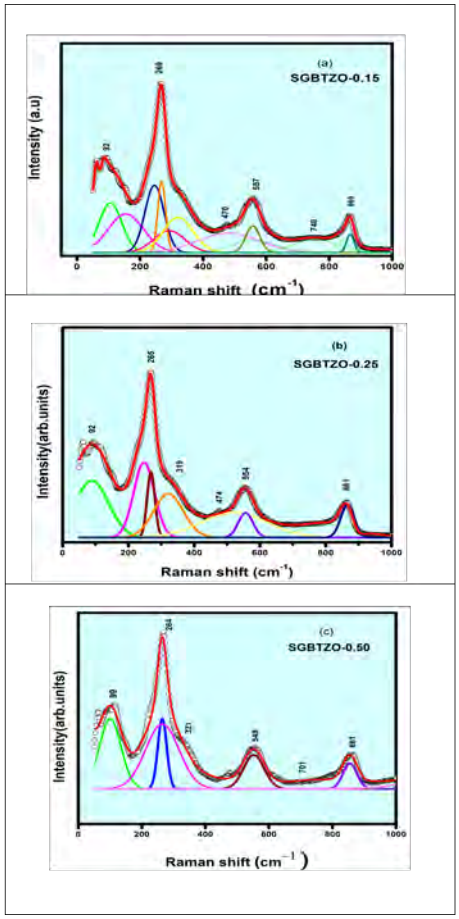

Fig 3. (a-c) Raman spectrum of SGBTZO-x (x=0.15, 0.25, 0.50)

The most effective technique to analyses the relaxation process observed in perovskite materials is impedance spectra. Impedance data was obtained at different temperatures in a broad frequency range of 1000Hz to 1MHz. Impedance spectroscopic data gives information about to characteristic relaxation properties of the samples and also provide information about the resistive and reactive parts of impedance. From this one can understand the microstructure and transport mechanism of the samples.

Nyquist plots for the SGBTZO-x samples drawn at various temperatures in the frequency range of 100 Hz to 1 MHz are displayed in inset Figure 4**(a-c).** The centers of the semicircular arcs lie below the real (Z') axis. The statistical distribution of relaxation time can be explained by depressed semicircles. The characteristics of the electrical response can be understood

by fitting the data into two semicircles. The first caused by the grain and the second by the existence of the grain boundary. The equivalent RC-circuit can be used to describe the underlying conduction mechanism. The experimental data fits with the theoretical curve. In the present investigation Z-view software was used and the parameter resistance and capacitance of grain and grain boundary were calculated at higher and lower frequency side of the semicircles. The grain and grain boundary resistances of all samples of SGBTZO-x are listed in Table 2.

Table 2. The grain and grain resistances of SGBTZO-x (where x=0.15, 0.25, 0.50)

Sample name	Grain resistance (Ω)	Grain capacitance (F)	Grainboundary resistance (Ω)	Grain boundary capacitance (F)
SGBTZO-0.15	5040	3.1E-9	2950	2.2E-5
SGBTZO-0.25	8920	1.5E-9	6000	1.8E-5
SGBTZO-0.50	102000	4.76E-10	91000	2.6E-5

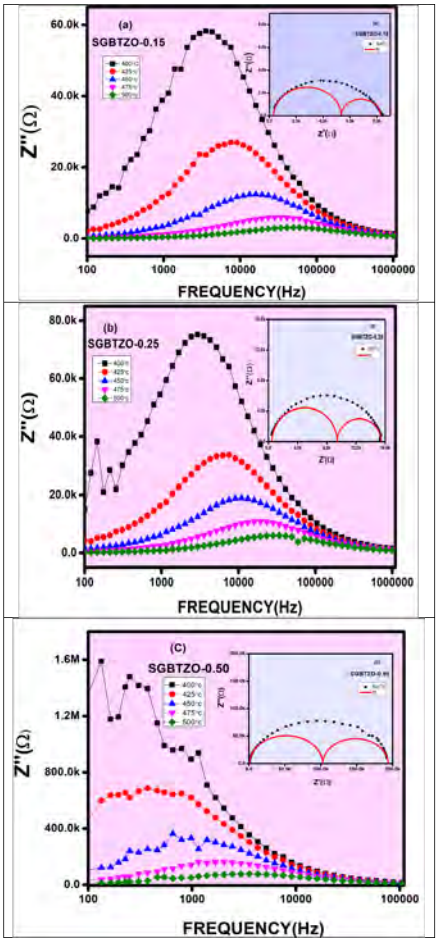

Fig 4. (a-c) Frequency dependence of the imaginary part of impedance for SGBTZO-x (x=0.15, 0.25, 0.50) at 400–500°C

Figure 4**(a-c)** shows variation of $Z^{//}$ (imaginary part of impedance) as a function of frequency for all samples. From the plots it is evident that $Z^{//}$ maximum is found to shift towards the right-hand side with the increase temperature. Moreover, the asymmetric broadening depends on the temperature and cooperation of the samples. The broad peaks also indicate the presence of multiple relaxation processes. More broadness observed at high temperature clearly indicates that grain-interface relaxation process predominates[10–13].

Figure 5**(a-c)** shows the variation of dielectric constant (marked as solid circles) and dielectric loss (marked as open circles) with temperature for all SGBTZO-x. Dielectric data has not shown any peak, except SGBTZO-0.50. A significant broad

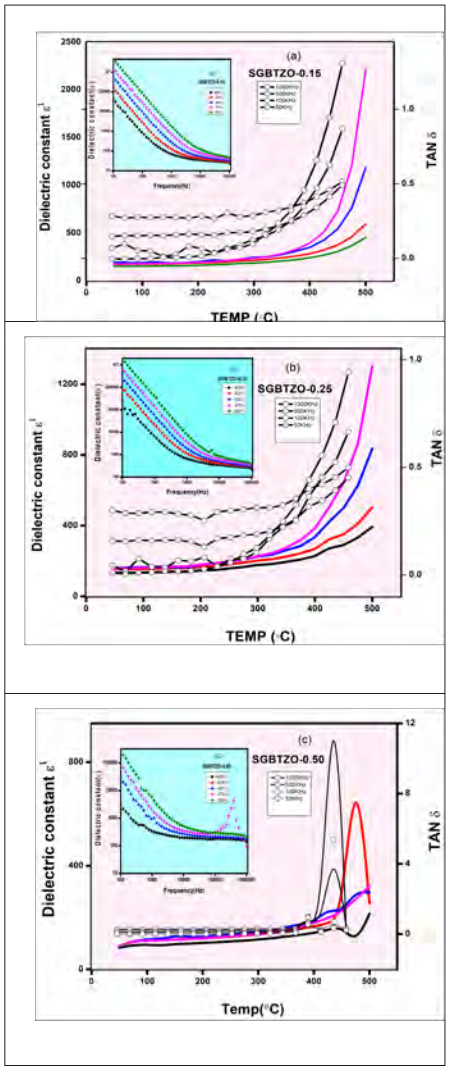

Fig 5. (a-c) Temperature dependence of dielectric constant and dielectric loss of SGBTZO-x (x=0.15, 0.25, 0.50)

peak indicates the diffuse phase transition temperature (DPT) of the sample. To understand the plausible reason, dielectric measurements were performed on the samples. The variation of ε' is found to decreases with increasing frequency. The frequency dependent and independent nature at lower and higher frequencies clearly indicates the ferroelectric transition nature of the samples

Figure 6**(a-c)** illustrates the fluctuation in AC conductivity of the synthesized SGBTZO-x material as a function of frequency at various temperatures. The conductivity plots can help to understand the transport behaviour of the layered perovskite materials. A dispersion observed at low frequency region demonstrates the presence of oxygen vacancy defects. At low-frequency region, vacancies defects are more active and act as a barrier to grain growth in ferroelectric phases. In the low frequency range, the AC conductivity curves are frequency independent and conductivity is found to increase linearly with temperature and frequency.

DC-conductivity was calculated by extrapolating AC-conductivity to 1Hz frequency. The variation of DC-conductivity with inverse temperature is shown as inset Figure 6 (**a-c**). According to Jonscher's law, the ac conductivity can be expressed as

$$\sigma\, ac = \sigma\, dc \left[1 + \left(\frac{\omega}{\omega_H}\right)^n\right]$$

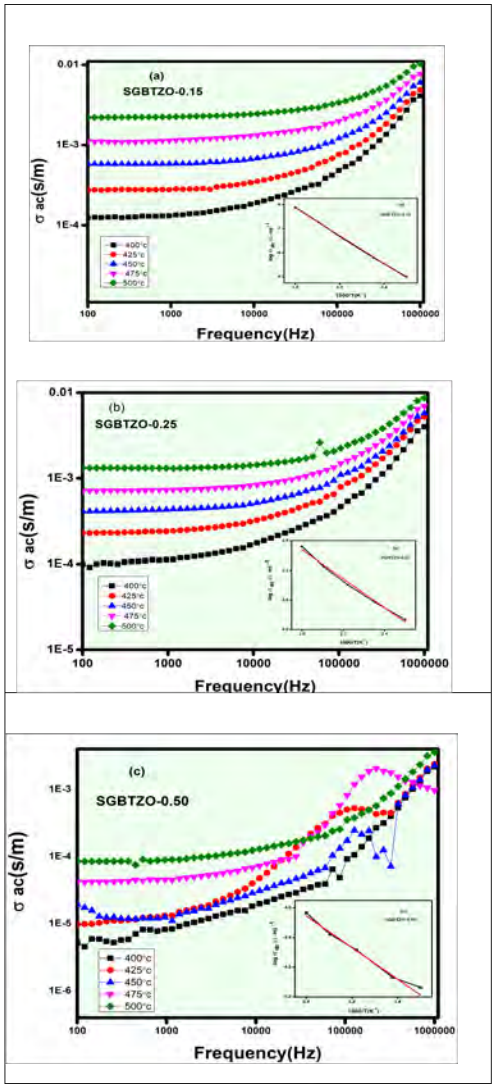

Fig 6. (a-c) Frequency dependence of AC-conductivity of SGBTZO-x (x=0.15, 0.25, 0.50) at 400–500°C.

Here the term 'n' represents exponent form, which dimensionless quantity. ω_H is called hopping frequency of charge carriers. These charge carriers move through localized regions separated by energy barriers, having different heights. The value of n explains many body interactions among the charge carriers and defects.[12,13]. A sudden change observed in the AC-conductivity data (Figure 6) indicates the transition temperature of the sample SGBTZO-0.50. From this one can speculate that the incorporation of Gd^{+3} ion in $(Bi_2O_2)^{2+}$ layers alter the electrical conductivity and decreases the space charge composition in bismuth oxide layers.

4 Conclusions

Gadolinium modified SBTZ polycrystalline ceramics were prepared by solid state route. X- ray diffraction data has shown single phase and the lattice parameters were calculated based on the parent compound. This study explores the effect of Gd^{+3}doping at Bi^{+3} in the layered perovskite Aurivillius family of SBTZ-x. This study provides two basic concepts on electrical properties and this could be helpful for tailoring the new multifunctional devices. A pronounced shift observed in the strong Raman modes clearly confirms that Gd^{+3} ion replaces the Bi^{+3} ion of A-site of layered- perovskite block. Dielectric data has shown the transition temperature of 450°C for SGBTZO-0.50. Detailed AC- conductivity data was found to fit with Jonscher's law. Based on the conductivity data, the conduction process changes from localized hopping to free ion migration, and it is thermally

activated process. Broad impedance spectroscopic and complex impedance plots show non-Debye relaxation.

References

1) Islam S, Khatun N, Habib MS, F UFS, I TN, A ASM, et al. Effects of yttrium doping on structural, electrical and optical properties of barium titanate ceramics. *Heliyon*. 2022;8(9):10529–10529. Available from: https://doi.org/10.1016/j.heliyon.2022.e10529.
2) Dhanya SR, Satapathy J. Structural, dielectric and impedance analysis of Nd doped $BiFeO_3$ prepared using solid-state synthesis method. *J Mater Sci: Mater Electron*. 2023;(5):34–34. Available from: https://doi.org/10.1007/s10854-023-09878-7.
3) Reaney IM, Damjanovic D. Crystal structure and domain-wall contributions to the piezoelectric properties of strontium bismuth titanate ceramics. *J App Phys*. 1996;80(7):4223–4225. Available from: https://doi.org/10.1063/1.363301.
4) Ramulu N, Prasad G, Suryanarayana S, Sankaram TB. Studies on electrical properties of $SrBi_4Ti_{4-3x}Fe_{4x}O_{15}$. *Bulletin of Material Science*. 2000;23(80(7)):431–437. Available from: https://www.ias.ac.in/article/fulltext/boms/023/05/0431-0437.
5) Nayak P, Singh AK. Correlation between orthorhombic distortion with relaxation and Conduction mechanism of Gd_{3+} modified $SrBi_4Ti_4O_{15}$. *Ceram Int*. 2018;44:22840–22849. Available from: https://doi.org/10.1016/J.CERAMINT.2018.09.076.
6) Sharma VK, Nathawat R, Rathore SS. Dielectric properties correlation with microstructure in $ABi_4Ti_4O_{15}$ (A = Sr, Ba) bismuth layered ferroelectrics. *Mat Adv*. 2022;3:4890–4898. Available from: https://doi.org/10.1039/D2MA00333C.
7) Tarasova N. Layered Perovskites $BaLnnInnO_{3n+1}$ (n = 1, 2) for Electrochemical Applications: A Mini Review. *Membranes*. 2023;13(34). Available from: https://doi.org/10.3390/membranes13010034.
8) Kennedya JB, Zhouiandarb Q, Kubotac Y, Katod K. Cation disorder and phase transitions in the four-layer ferroelectric Aurivillius phases $ABi_4Ti_4O_{15}$ (A = Ca, Sr, Ba, Pb). *J Solid State Chem*. 2008;181:1377–1386. Available from: https://doi.org/10.1016/j.jssc.2008.02.015.
9) Jyothirmai C, Malathi A, Kirana K, Prasad G, Prasad NV. Impedance spectroscopic Studies on Sr and Zr modified four layered BLSF ceramics. *Materials Today: Proceedings* . 2023;((92)):1213–1217. Available from: https://doi.org/10.1016/j.matpr.2023.05.319.
10) Raman EV, Graça MPF, Valente MA, Sankaram TB. Improved ferroelectric and pyroelectric properties of Pb-doped $SrBi_4Ti_4O_{15}$. Ceramics for high temperature applications, . *Alloys and Comp*. 2014;(583):198–205. Available from: https://doi.org/10.1016/j.jallcom.2013.08.181.
11) Jose R, Vineetha P, Rafiq MA, Saravanan VK. Investigation into defect chemistry and relaxation processes in niobium doped and undoped $SrBi_4Ti_4O_{15}$ using impedance spectroscopy. *RSC Advances*. 2018;(8). Available from: https://doi.org/10.1039/C8RA06621C.
12) Nayak P, Badapanda T, Singh AK, Panigrahi S. Possible relaxation and conduction Mechanism in W^{6+}doped $SrBi_4Ti_4O_{15}$ ceramic. *Ceram Int*. 2017. Available from: https://doi.org/10.1016/j.ceramint.2016.12.105.
13) Babu B, Prasad G, Kumar GS, Prasad NV. Studies on samarium modified $SrBi_4Ti_4O_{15}$ Aurivillius ferroelectric ceramics. *Ferroelectrics*. 2021. Available from: https://doi.org/10.1080/00150193.2020.1868876.